

Nucleation of “Hut” Pits and Clusters during Gas-Source Molecular-Beam Epitaxy of Ge/Si(001) in *In Situ* Scanning Tunneling Microscopy

I. Goldfarb, P. T. Hayden, J. H. G. Owen, and G. A. D. Briggs

University of Oxford, Department of Materials, Parks Road, Oxford OX1 3PH, England

(Received 18 February 1997)

Heteroepitaxial Ge/Si(001) growth has been investigated using *in situ* scanning tunneling microscopy. While at 620 K the epitaxial strain is relieved by formation of three-dimensional islands (so-called “hut” clusters), at 690 K the strain is first relieved by hut pits, having the cluster shapes but with their apex pointing down. Although predicted theoretically to have lower energy than clusters, hut pits have never been observed individually before. Details of cluster and pit nucleation are also presented for the first time. [S0031-9007(97)03197-9]

PACS numbers: 81.15.Kk, 61.16.Ch, 68.35.Bs, 68.65.+g

Ge on Si is a model Stranski-Krastanow growth system, where the initial two-dimensional (2D) wetting layer grows pseudomorphically until the strain due to the 4.2% lattice mismatch is eventually relaxed via formation of three-dimensional (3D) macro islands [1–3]. The kinetic route for strain relaxation passes through a series of rather complex surface phase transitions, before reaching the final state of large 3D islands, fully relaxed by dislocations [4]. A particularly important stage of these transitions is the formation of small, fully coherent 3D islands which, because of their small dimensions, can exhibit the electron confinement properties of quantum dots. With their rectangular (100)-type bases and hutlike shapes formed by {501}-type facets, these were called “hut” clusters by Mo *et al.*, who were the first to reveal them in their STM images [5]. Since then the hut clusters have been identified and characterized by other investigators, using STM [6,7], AFM [8], TEM [3], and a variety of diffraction techniques [9–11].

In this Letter we describe real-time elevated-temperature-scanning-tunneling-microscopy (ET-STM) observation of gas-source-molecular-beam-epitaxy (GS-MBE) growth of Ge on Si(001) from GeH₄. Voigtländer and Zinner [12] were the first to use *in situ* STM during solid-source MBE of Ge/Si(111), and have convincingly shown the advantages of the real-time STM observations over the more conventional “growth interruption-observation” method. The presence of hydrogen on the surface in the GS-MBE process provides an additional growth parameter, which can be utilized to improve the quality of the growing film. It is also known that the sequence of surface phase transitions during Ge growth on Si(001) differs from that on the Si(111) [12]. Thus using our method, we have been able to observe certain growth characteristics which were never observed before, to support some of the previous conjectures and to propose new ones.

A JEOL ET-STM, equipped with *in situ* reflection high-energy electron diffraction (RHEED), and capable of operation up to 1200 °C was used. The images were taken

using electrochemically etched W tips, during exposure to germane at 620 and 690 K growth temperatures (achieved by direct current resistive heating and measured by an optical pyrometer with ± 30 K accuracy) in both “constant current” and “log *I*” modes, with currents around 0.1 nA and sample bias between ± 3 V. GeH₄ (99.99%) was fed through a precision valve onto the sample mounted in the STM stage and the tip was left to scan, while a desired constant pressure in the 10^{-7} – 10^{-5} Pa range was maintained.

As has been well established, the first phase transition of the Ge covered Si(001) surface is the (2×1) to $(2 \times N)$ transition, when the Ge coverage is about one monolayer [4,13]. The second, $(2 \times N)$ to $(M \times N)$ transition has also been observed by several groups [4,6,13]. This “patched” or “grooved” structure consists of dimer vacancy lines (DVLs) and dimer-row vacancies (DRVs), forming a two-dimensional $(M \times N)$ grid on the surface (see Fig. 1), allowing for more strain relaxation and delaying the 2D to 3D transition. However, since the separation between the DVLs, as well as between the DRVs, does not decrease beyond a certain value (in this work $7a$ and $9a$, respectively, where $a = 3.84$ Å is the Si surface lattice constant) due to repulsive interaction between them [14], a new phase transition must take place to relieve the strain continuously evolving with coverage.

The strain can be further released by nucleation of misfit dislocations, but the kinetic barrier for dislocation nucleation increases rapidly with misfit [15]. Therefore, in the case of 4.2% mismatch between Si and Ge, the surface roughens to provide a partial strain relaxation by dilatation of lattice planes which are compressed in the 2D film, in spite of the increase in surface energy. In the particular case of Ge/Si(001) hut clusters, x-ray diffraction measurements revealed that although the cluster base is almost fully strained, towards the apex the strain is almost fully relaxed [11]. Negative hut clusters, i.e., hut pits, can relieve the strain in the same way. A full calculation shows that if the wetting layer is thick enough for pits to occur, they will always have a lower energy than a cluster of the

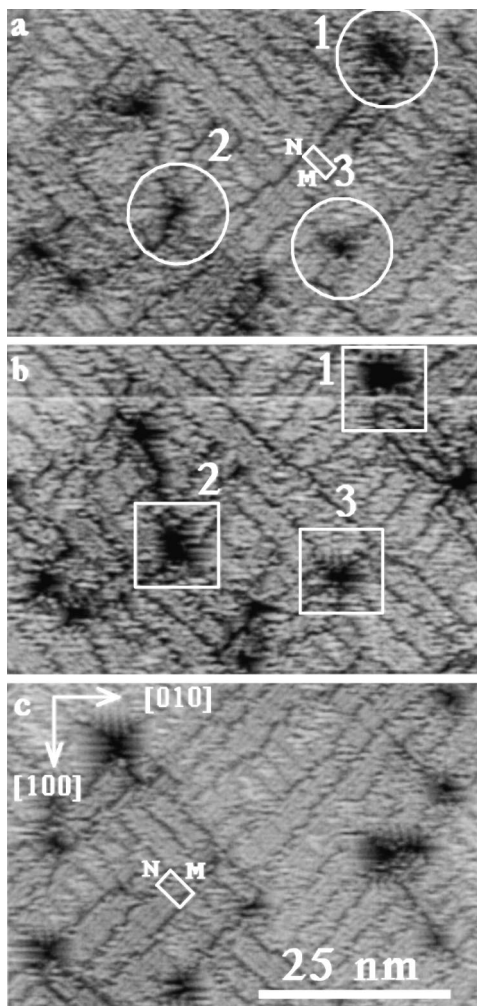


FIG. 1. (a) Voids in the Ge wetting layer to be transformed into pits. ($M \times N$) unit cell is outlined. (b) Conversion of the voids [encircled in (a)] into pits (boxed). (c) Well defined pits with $\langle 100 \rangle$ basis and $\{501\}$ facets.

same size and shape [15]. Figure 1(b) shows precisely this case. Prior to this work hut pits have never been observed individually, but only in combination with hut clusters [8]. At least one of the reasons for that is the short existence range of hut pits, between 7.7 and 8.3 ML at 690 K. Hut pits nucleate heterogeneously from the existing defects, mostly voids formed by agglomeration of missing dimers, such as those shown in Fig. 1(a). Figure 2 shows the dependence of void size on the Ge coverage. The “knee” indicates the critical size and coverage for a stable hut pit from which the pits grow spontaneously, and corresponds to the transition from shapeless voids encircled in Fig. 1(a) to hut pits boxed in Fig. 1(b).

Figure 3 shows a typical sequence from our growth movie, taken at 620 K, which demonstrates the main stages of cluster nucleation. The flat appearance of the clusters in Fig. 3 (and in Fig. 4) was caused by high-contrast STM conditions for better monitoring of the wetting layer. The 11° line splitting in $[010]$ RHEED patterns [9,10] [inset of Fig. 5(c)] confirmed the existence of the $\{501\}$

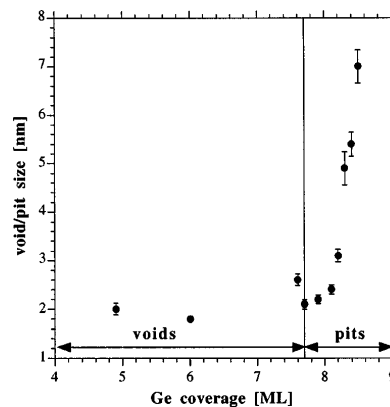


FIG. 2. Void size dependence on coverage, indicating the critical point for the void-to-pit transformation. The bars represent the statistical error.

facets. As can be seen by comparison of Fig. 3(a) to Fig. 3(b), the shapeless, curved edges of the void (marked “X”) transform into straight $\langle 100 \rangle$ -oriented edges, as a precursor to the nucleation [Fig. 3(c)] and growth of a hut cluster, as appears in Fig. 3(d). Figure 4 shows the Ge wetting layer before and after cluster nucleation at 620 K. It is apparent from comparison between Figs. 4(a) and 4(b) that every nucleation event took place on surface irregularities, such as steps or voids numbered 1–6 in

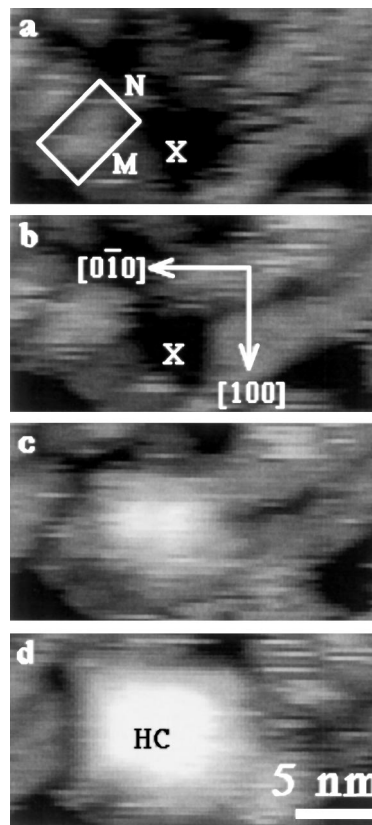


FIG. 3. Hut cluster nucleation on void (marked “X”) $\langle 100 \rangle$ -type edges. (a) The initial void, (b) formation of the $\langle 100 \rangle$ -edges, (c) nucleation, and (d) nucleus growing into a hut cluster (HC). Wetting layer thickness is between 3 and 4 ML.

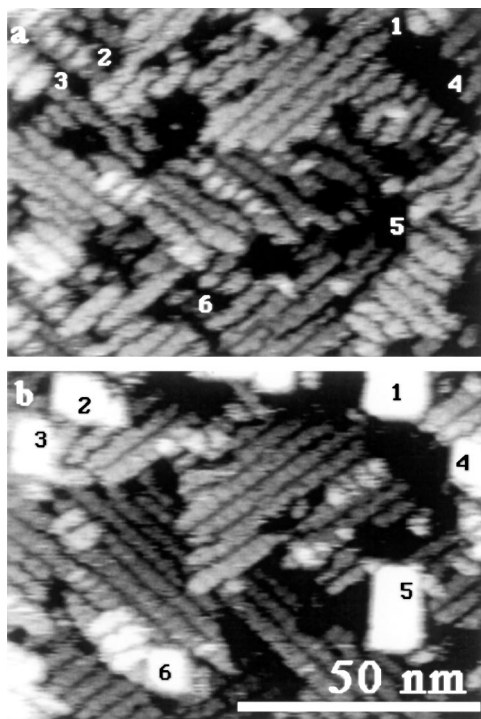


FIG. 4. (a) Typical surface of Ge wetting layer prior to cluster nucleation at 620 K. (b) The same surface as in (a), after hut cluster nucleation. Note the correspondence between the 1–6 cluster locations and the 1–6 nucleation sites at surface irregularities in (a).

Fig. 4(a), prior to which irregularities transformed into straight $\langle 100 \rangle$ segments, leaving the flat portions of terraces free of nuclei. These experimental results fully support the mechanism, previously proposed by Mo *et al.*, namely, that $\langle 100 \rangle$ -type step edges serve as the nucleation sites for hut clusters [5]. At this temperature Ge initially grows predominantly by island formation on the Si terraces, leading to relatively rough multilayer growth, i.e., high density of nucleation centers and, eventually, to a rather dense and random cluster disposition, as can be seen, for example, in Fig. 5(c). It follows from our experimental results that, contrary to previous belief [3], homogeneous cluster nucleation does not occur even at temperatures as low as 620 K. The dense and random cluster disposition observed at low temperatures may cause an impression of homogeneous nucleation, when observed *ex situ* or with a less surface-sensitive technique [3].

At 690 K only the first nucleation stages take place [see Figs. 3(a) and 3(b)], and the process continues with the formation of straight $\langle 100 \rangle$ -oriented void edges, leading to a formation of pits instead of clusters (see Fig. 1). Numerous events of this kind were observed by us, when the thickness of the wetting layer had exceeded 7.7 ML. This wetting layer was thick enough to accommodate a pit, and hence our results are in excellent agreement with theoretical predictions of Tersoff and LeGoues [15]. As higher growth temperatures result in thicker wetting layers

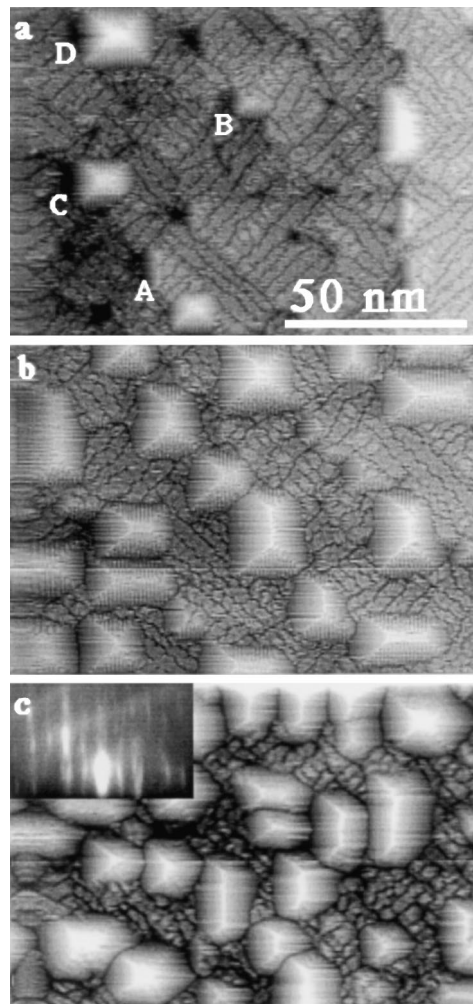


FIG. 5. (a) Beginning of the “pit-to-cluster” transformation at 690 K. Note also cluster nucleation on the long $[100]$ step edge. (b) Step decoration by cluster “necklaces” at later stages of growth at 690 K. (c) Typical appearance of the Ge hut clusters grown at 620 K. The $[010]$ RHEED pattern is shown in the inset.

[16] and pits can only form at sufficiently thick wetting layers, pits only form at adequately high temperatures. This also means that the thickness of the wetting layer is the major factor that determines whether hut pits or hut clusters form. As further growth causes a replacement of pits by clusters, as described in the next paragraphs, and since at this temperature the Ge is predominantly incorporated at step edges, this ultimately leads to decoration of steps by hut clusters, as appears in Figs. 5(a) and 5(b).

Hut clusters eventually succeed the pits, since the pit capability to accommodate strain is limited by its smaller maximal size. Although square-based pyramids are the most energetically favored cluster shapes, their often elongated appearance has led Jesson *et al.* to propose a model explaining island-shape instabilities by nucleation and growth on the $\{501\}$ facets of hut clusters [8]. Our *in situ* observations prove that growth on $\{501\}$ facets is indeed the most common mechanism of cluster elongation. Figures 6(a)–6(c) capture elongation of the initially

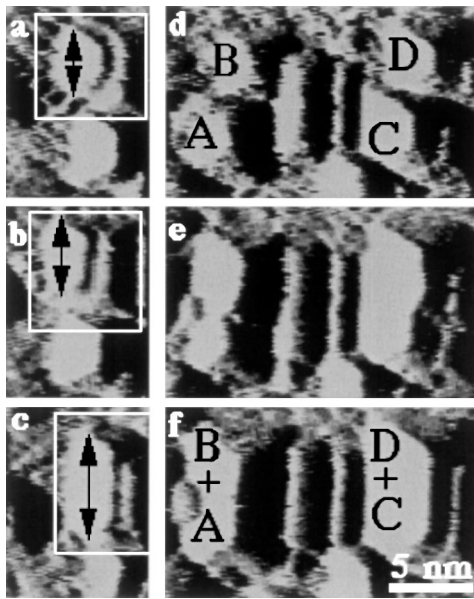


FIG. 6. (a)–(c) “log I ” STM image of facial island growth. The elongation direction and the magnitude are indicated. (d)–(f) Coalescence of two pairs of neighboring clusters, A-B and C-D, leading to the twice longer appearance of the final clusters.

square-based hut cluster (boxed), simultaneously with growth of 2D island (marked by an arrow) on one of its $\{501\}$ facets.

Some of the elongated cluster shapes are caused by coalescence of neighboring clusters, when they are sufficiently close to each other as the two pairs of neighbors (A-B and C-D) shown in Figs. 6(d)–6(f). Clearly, the excessive surface energy of the facets on each side of the boundary line between them [two facets for each pair in Fig. 6(d)] can be eliminated by gradually filling the gap with incoming flux [Fig. 6(e)], leading to full coalescence and the elongated shape in Fig. 6(f). Governed by the same rules, pits can also coalesce when sufficiently close to each other. Two examples of this happening are shown in Fig. 7. However, as can be judged from Figs. 1 and 5(a), this is seldom the case. Pit growth analogous to the facial cluster growth would be by the agglomeration of vacancies on the pit facet, or in other words, by the transfer of material from the facets to the flat regions between the pits. Since the critical 2D layer thickness is exceeded, this transferred material immediately forms 3D clusters. Cluster nucleation by such a process can be seen in regions “A” and “B” in Fig. 5(a), and the resulting fully developed clusters in regions “C” and “D.” Since the incoming germanium tends to fill the pits, the clusters gradually overtake them, leading to a cluster-dominated surface shown in Fig. 5(b).

In conclusion, we have monitored the surface evolution during the GS-MBE Ge growth on Si(001), with *in situ* ET-STM. This method has enabled us to observe the initial stages of each surface phase transition in the complex

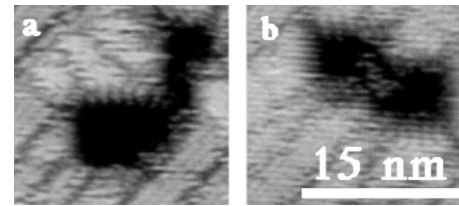


FIG. 7. (a),(b) Coalescence of neighboring hut pits.

series, determined by the kinetic pathway to strain relief during the heteroepitaxy. Following these observations we have experimentally proved two important, previously proposed theoretical models: Tersoff’s model that favors pits over clusters, provided the wetting layer is thick enough, and Jesson’s model which accounts for cluster shape instabilities. Our growth experiments at 690 K, and sufficiently thick wetting layer yielded formation of hut pits instead of hut clusters, although during growth at 620 K (and thinner wetting layer) only hut clusters were observed to form. The clusters grow predominantly in a facet-nucleation and growth mode, but also by coalescence. We have also observed for the first time heterogeneous nucleation of pits and clusters on surface irregularities with $\langle 100 \rangle$ -type straight edges, and proposed a plausible explanation for the succession of pits by clusters: Having formed and relieved some strain, as dictated by thermodynamics, pits are eventually replaced by clusters due to the kinetic nature of the growth process. Although at both temperatures the cluster nucleation is heterogeneous, with $\langle 100 \rangle$ -type edges as a precursor, at 620 K the cluster distribution is more random than at 690 K, where clusters predominantly decorate step edges in a form of continuous “necklace,” indicating the fascinating possibility of creating self-assembled quantum wires, as well as quantum dots.

This work is supported by EPSRC (GR/K08161).

- [1] D. J. Eaglesham and M. Cerullo, Phys. Rev. Lett. **64**, 1943 (1990).
- [2] D. J. Eaglesham and M. Cerullo, Mater. Sci. Eng. B **30**, 197 (1995).
- [3] M. Hammar *et al.*, Surf. Sci. **349**, 129 (1995).
- [4] M. Tomitori *et al.*, Appl. Surf. Sci. **76/77**, 323 (1994).
- [5] Y.-W. Mo *et al.*, Phys. Rev. Lett. **65**, 1020 (1990).
- [6] J. Knall and J. B. Pethica, Surf. Sci. **265**, 156 (1991).
- [7] M. Tomitori *et al.*, Surf. Sci. **301**, 214 (1994).
- [8] D. E. Jesson, K. M. Chen, and S. J. Pennycook, Mater. Res. Bull. **21**, 31 (1996).
- [9] C. E. Aumann, Y.-W. Mo, and M. G. Lagally, Appl. Phys. Lett. **59**, 1061 (1993).
- [10] N. Ohshima *et al.*, Appl. Phys. Lett. **63**, 3055 (1993).
- [11] A. J. Steinfort *et al.*, Phys. Rev. Lett. **77**, 2009 (1996).
- [12] B. Voigtländer and A. Zinner, Appl. Phys. Lett. **63**, 3055 (1993).
- [13] U. Köhler *et al.*, Ultramicroscopy **42–44**, 832 (1991).
- [14] X. Chen *et al.*, Phys. Rev. Lett. **73**, 850 (1994).
- [15] J. Tersoff and F. K. LeGoues, Phys. Rev. Lett. **72**, 3570 (1994).
- [16] I. Goldfarb *et al.* (to be published).